JOURNAL OF MATERIALS SCIENCE **40** (2005) 889–893

A new model for radiation-induced grain boundary segregation with grain boundary movement in concentrated alloy system

N. SAKAGUCHI*
Center for Advanced Research of Energy Conversion Materials, Hokkaido University, Sapporo 060-8628, Japan
E-mail: sakagu@ufml.caret.hokudai.ac.jp

S. WATANABE
Department of Materials Science, Graduate School of Engineering, Hokkaido University, Sapporo 060-8628, Japan

H. TAKAHASHI
Center for Advanced Research of Energy Technology, Hokkaido University, Sapporo 060-8628, Japan

We have developed a new model for radiation-induced grain boundary migration (RIGM) and radiation-induced segregation (RIS) for austenitic iron-chromium-nickel alloy system. It was assumed that the RIS was induced by diffusional and annihilation processes of excess point defects at the grain boundary, and the RIGM occurred due to rearrangement process of atoms on one of the interfacial planes by annihilation of point defects. The calculated results indicated that the region of RIS was enlarged by the RIGM and asymmetrical concentration profiles were observed around the migrated grain boundary. The present model could explain the RIS behavior with or without grain boundary migration as comparing with our previous experimental results.

1. Introduction

Under irradiation, solute redistribution in concentrated alloys occurs because of the preferential interaction between the solute atoms and excess point defects moving toward sinks, such as surface or grain boundaries. In austenitic stainless steels, i.e. a type 304 which are used a light-water reactor components [1, 2], radiation-induced segregation (RIS) near grain boundaries and radiation-induced grain boundary migration (RIGM) cause significant deleterious effects to their mechanical and chemical properties [3]. The seriousness of this problem has been considered as irradiation-assisted stress corrosion cracking (IASCC) induced by the RIS [4, 5]. It is thus important to investigate the mechanism for retardation of radiation-induced solute redistribution and behavior of grain boundary movement under irradiation.

In last ten years, we have proposed a model for RIS around a moving grain boundary in austenitic iron-chromium-nickel ternary alloy systems and the results of calculations agreed with experimental results well for the RIS [6–8]. We have also reported about the atomistic observation of grain boundary structural changes which were induced by the RIGM during electron irradiation and it was indicated that the grain boundary movement occurred by a rearrangement process of atoms on one of the interfacial planes to another plane due to mutual annihilation of excess point defects around there [9, 10].

In the present paper, we shall propose a new RIS model with the RIGM based on diffusion and reaction-rate equations. The model is including the rearrangement process of a boundary interfacial plane as the RIGM kinetics. To clarify the validity of the present model, we compared the calculated results with our previous results for the RIS and the RIGM in an austenitic stainless steel during the electron irradiation.

2. Simulation method

Simultaneous solutions to diffusion and reaction-rate equations describe solute segregation induced by excess vacancy and interstitial fluxes to a grain boundary and by solute-defects interaction [11–13]. We also consider the movement of the grain boundary by the rearrangement of atoms on one of the interfacial planes to another plane due to the defect flows and annihilations toward the boundary interfacial planes.

*Author to whom all correspondence should be addressed.

The approach is to solve the diffusion and reaction-rate equations for point defects and alloy components to obtain the terms of coupling the defect and solute fluxes. It is also noticeable that the equations are described with a relative system of coordinates for the grain boundary. The continuity equations are

$$\frac{dC_k}{dt} = \frac{\partial}{\partial x}\left[D_k\frac{\partial C_k}{\partial x} - C_k\left(d_k^v\frac{\partial C_v}{\partial x} - d_k^i\frac{\partial C_i}{\partial x}\right)\right] - v_{gb}\frac{\partial C_k}{\partial x} \quad (k = \text{Fe, Cr, Ni}) \quad (1)$$

$$\frac{dC_v}{dt} = \frac{\partial}{\partial x}\left[D_v\frac{\partial C_v}{\partial x} - C_v\sum_k d_k^v\frac{\partial C_k}{\partial x}\right] + G_{dpa} - R_{vi}D_iC_vC_i - z_v\rho D_v\left(C_v - C_v^{th}\right) - v_{gb}\frac{\partial C_v}{\partial x} \quad (2)$$

$$\frac{dC_i}{dt} = \frac{\partial}{\partial x}\left[D_i\frac{\partial C_i}{\partial x} + C_i\sum_k d_k^i\frac{\partial C_k}{\partial x}\right] + G_{dpa} - R_{vi}D_iC_vC_i - z_i\rho D_iC_i - v_{gb}\frac{\partial C_i}{\partial x}. \quad (3)$$

In above equations, solute species (iron, chromium or nickel) are identified by the index, k, and vacancies and interstitials are represented by v and i, respectively. The last terms in each equation are the drift terms due to the RIGM, and v_{gb} is a velocity of grain boundary motion as discussed in later. The other important parameters here are the coupling parameters, d_k^v and d_k^i which are the partial diffusivities of alloying elements via vacancies and interstitials, determined by

$$d_k^{v,i} = a_0^2\nu_k^{v,i}\exp\left(-\frac{E_{v,i}^m}{k_BT}\right) \quad (4)$$

where $\nu_k^{v,i}$ are the vibration frequencies of k-atom around a vacancy and interstitial, a_0 is the lattice constant, and $E_{v,i}^m$ are the migration energies of point defects, respectively. The diffusion coefficients of point defects and the radiation-enhanced diffusivities of atoms are then given by

$$D_{v,i} = \sum_k d_k^{v,i}C_k \quad (5)$$

$$D_k = d_k^vC_v + d_k^iC_i. \quad (6)$$

Other parameters shown are the displacement rate, G_{dpa}, mutual recombination coefficient, R_{vi}, internal dislocation density, ρ, bias factors of the dislocation for point defects, $z_{v,i}$, and the thermal equilibrium concentration of vacancies, C_v^{th}, respectively.

At the grain boundary, we additionally defined the effective recombination sites for the point defects as

$$\frac{dC_v}{dt} = G_{gb}^v + S_{gb}D_v\left(C_v - C_v^{th}\right) - v_{gb}\frac{\partial C_v}{\partial x} \quad (7)$$

$$\frac{dC_i}{dt} = G_{gb}^i + S_{gb}D_iC_i - v_{gb}\frac{\partial C_i}{\partial x} \quad (8)$$

where S_{gb} is the area number density of the recombination sites on the boundary interface, and $G_{gb}^{v,i}$ are the generation rates of point defects by diffusion of the point defects toward the boundary interface written as

$$G_{gb}^{v,i} = \frac{1}{d_{gb}}\left[-D_{v,i}\frac{\partial C_{v,i}}{\partial x} \pm C_{v,i}\sum_k d_k^{v,i}\frac{\partial C_k}{\partial x}\right]_{x=X_{gb}-\frac{d_{gb}}{2}} - \frac{1}{d_{gb}}\left[-D_{v,i}\frac{\partial C_{v,i}}{\partial x} \pm C_{v,i}\sum_k d_k^{v,i}\frac{\partial C_k}{\partial x}\right]_{x=X_{gb}+\frac{d_{gb}}{2}} \quad (9)$$

where d_{gb} is the width of the grain boundary and X_{gb} is the position of the boundary plane as schematically illustrated in Fig. 1. The parameter, S_{gb}, is fixed as functions of misorientation angle and Σ value to reproduce the experimental RIS data on various kinds of grain boundaries [14]. Finally, the velocity of grain boundary motion is described as follows

$$v_{gb} = d_{gb}S_{gb}\left[\alpha_vD_v\left(C_v - C_v^{th}\right) + \alpha_iD_iC_i\right] \quad (10)$$

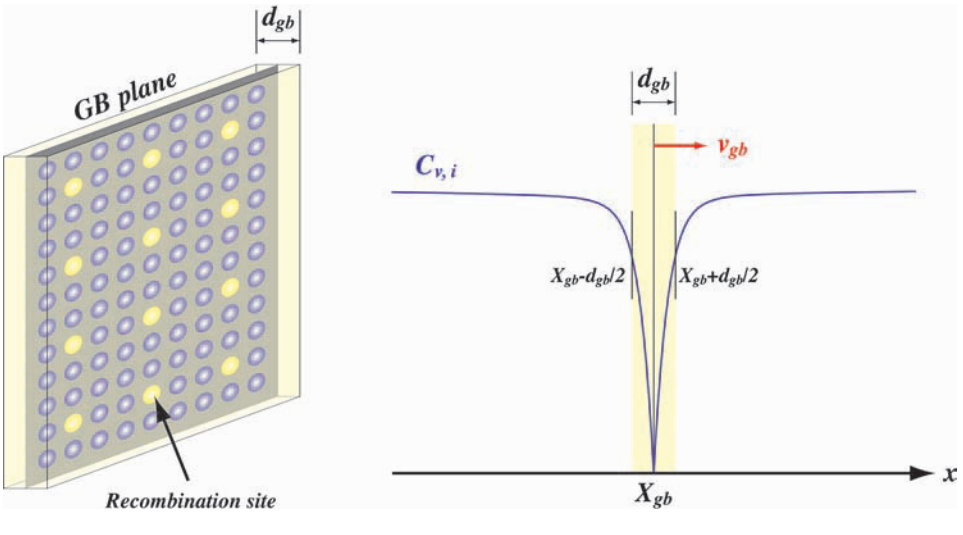

Figure 1 Schematic illustration about the parameters, S_{gb} and $G_{gb}^{v,i}$.

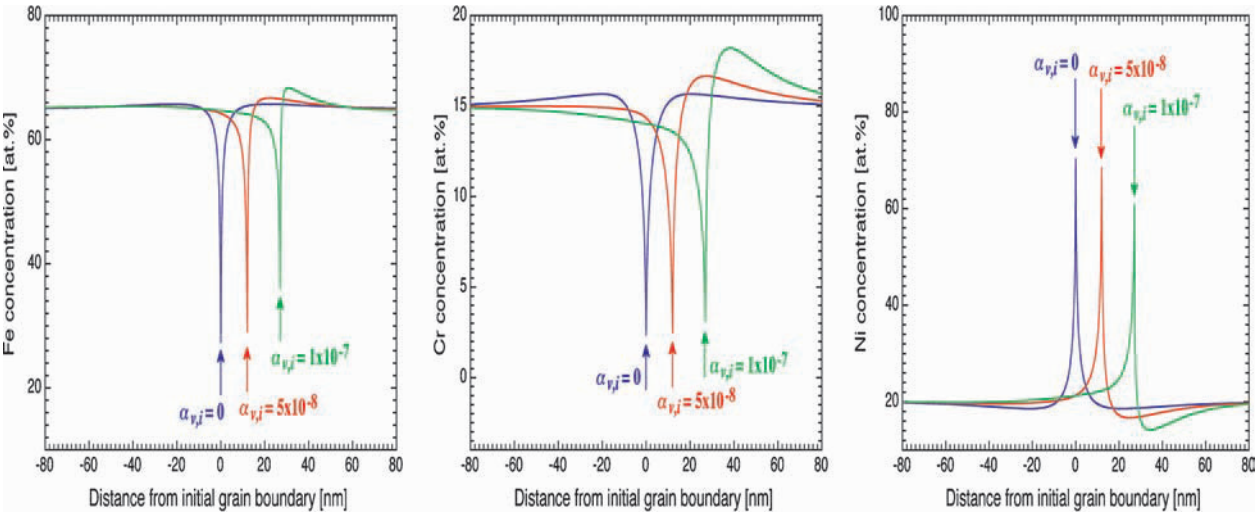

Figure 2 Concentration profiles after irradiation to 10 dpa at 2×10^{-3} dpa/s and at 623 K. The $\alpha_{v,i}$ values were 0, 5×10^{-8}, 1×10^{-7}, respectively.

where $\alpha_{v,i}$ are the fraction of the annihilating point defects which contribute to the rearrangement of atoms at a boundary interfacial plane. For the case of $\alpha_{v,i} > 0$, the grain boundary migration occurs with solute redistribution, and we can only calculate the RIS without the RIGM in the case of $\alpha_{v,i} = 0$. We chose low values for the rearrangement probability $\alpha_{v,i}$ (less than 1×10^{-7}) to reproduce the experimental RIGM behavior.

For the calculations, finite difference methods and numerical integration have been used to solve the coupled equations. The LSODE package of subroutines [15] was used for the numerical integration of stiff ordinary differential equations. The material constants used in the present calculations are listed in Table I.

3. Results and discussions

Fig. 2 shows typical results on grain boundary segregation with or without grain boundary migration for the cases of $\alpha_{v,i} = 0, 5 \times 10^{-8}$ and 1×10^{-7}. The displacement rate, irradiation dose and temperature were 2×10^{-3} dpa/s, 10.0 dpa and 623 K, respectively. The grain boundaries moved to right direction for $\alpha_{v,i} = 1 \times 10^{-8}$ and 1×10^{-7}, and the migration distances were 12 nm and 27 nm, respectively. It was evident that the distributions of alloying elements are not symmetric with respect to the migrated grain boundaries and that the segregation effect was more pronounced behind the migrating boundaries than ahead of these. Alternatively, nickel depletion and iron/chromium segregation were observed ahead of the migrated boundaries, It was also indicated that the migration distance and the deviation from symmetry increased with $\alpha_{v,i}$ value, although the magnitude of the RIS at the migrated boundaries decreased with the $\alpha_{v,i}$ value. In Fig. 3, we plotted relationships between the migration distance, the width of chromium deplete zone and the magnitude of $\alpha_{v,i}$. Here, we defined the chromium depleted zone as a region where chromium composition was less than 12%. The linear relationship between the migration distance and the $\alpha_{v,i}$ value was obtained, but the chromium depleted zone was expanded progressively in increases of the migration distance or the $\alpha_{v,i}$ value. The present results indicate that the irradiation-induced sensitization on the IASCC depletion will be enhanced by the grain boundary migration during the irradiation. Fig. 4 shows

TABLE I Main parameters used in the present calculations

Input parameter	Notation	Value
Vacancy jump frequency via Fe atom	ν^{v}_{Fe}	5.0×10^{13} s^{-1}
Vacancy jump frequency via Cr atom	ν^{v}_{Cr}	1.0×10^{14} s^{-1}
Vacancy jump frequency via Ni atom	ν^{v}_{Ni}	1.5×10^{13} s^{-1}
Vacancy migration energy	E^{m}_{v}	1.05 eV
Interstitial jump frequency	ν^{i}_{k}	5.0×10^{12} s^{-1}
Interstitial migration energy	E^{m}_{i}	0.85 eV
Formation enthalpy of vacancy	H^{f}_{v}	1.6 eV
Formation entropy of vacancy	S^{f}_{v}	1.5 k_B
Lattice constant	a_0	3.6×10^{-10} m
Bias factor of dislocation for vacancy	Z_v	1.0
Bias factor of dislocation for interstitial	Z_i	1.2
Dislocation density	ρ	10^{14} m^{-2}
Recombination factor	R_{vi}	$500/a_0^2$
Number density of recombination site at GB	S_{gb}	1×10^{20} m^{-2}
Grain boundary depth	d_{gb}	4×10^{-10} m

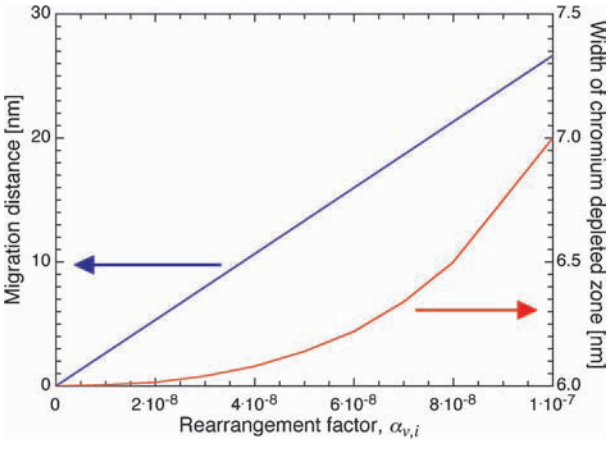

Figure 3 Dependencies of migration distance and width of chromium deplete zone on the magnitude of $\alpha_{v,i}$. The irradiation conditions were 10 dpa at 2×10^{-3} dpa/s and at 623 K.

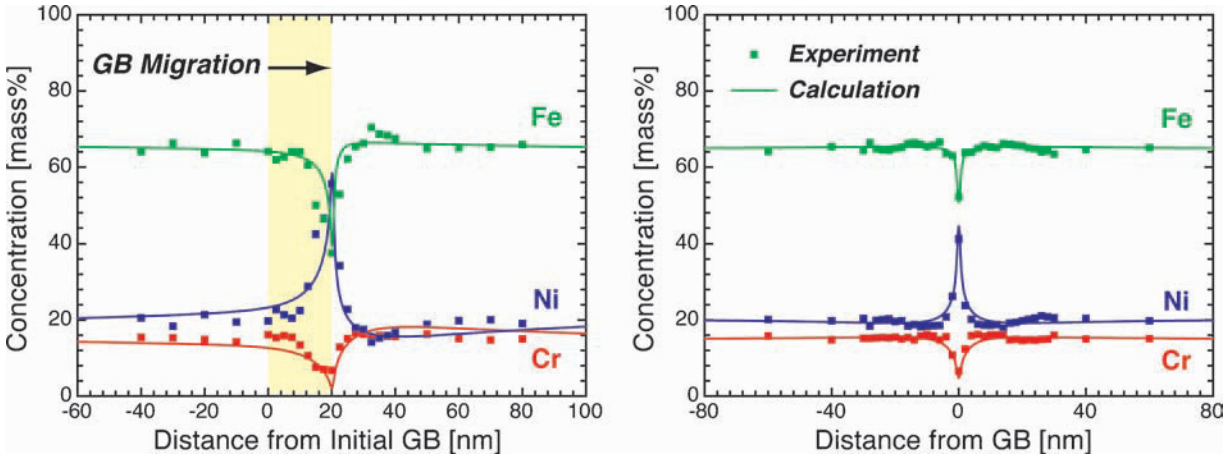

Figure 4 Concentration profiles after electron irradiation to 14.4 dpa at 4×10^{-3} dpa/s and at 623 K with or without grain boundary migration. Solid lines are calculated results with ($\alpha_{v,i}. = 1 \times 10^{-7}$) or without ($\alpha_{v,i}. = 0$, $S_{gb} = 1 \times 10^{19}$ m^{-2}) the grain boundary migration.

the distributions of alloying elements around the grain boundary with ($\alpha_{v,i} = 1 \times 10^{-7}$) or without ($\alpha_{v,i} = 0$, $S_{gb} = 1 \times 10^{19}$) the RIGM after electron irradiation to 14.4 dpa at 4×10^{-3} dpa/s and at 623 K. The experimental RIS data obtained by EDS analysis [10] were also plotted in the figure. We considered spatial distribution of electron probe by means of averaging the calculated concentration profiles with an EDS probe size distribution [8]. This technique is of importance for simulating the actual RIS data taken by TEM-EDS analysis. It was assumed that the mean EDS probe size was 1.0 nm. The overall agreement between the calculations and the experimental data is remarkably good. It indicates the validity of the present model for both RIS and RIGM. In Fig. 5, the calculated ($\alpha_{v,i} = 5 \times 10^{-8}$) and experimental concentration profiles on an identical grain boundary [14] are shown after electron irradiation to 1, 3, 5 and 10 dpa at 2×10^{-3} dpa/s and at 623 K. Both results show that the chromium depleted zone is expanded with increasing both of migration distance and irradiation dose. The deviations from symmetry of the concentration profiles were also enhanced with

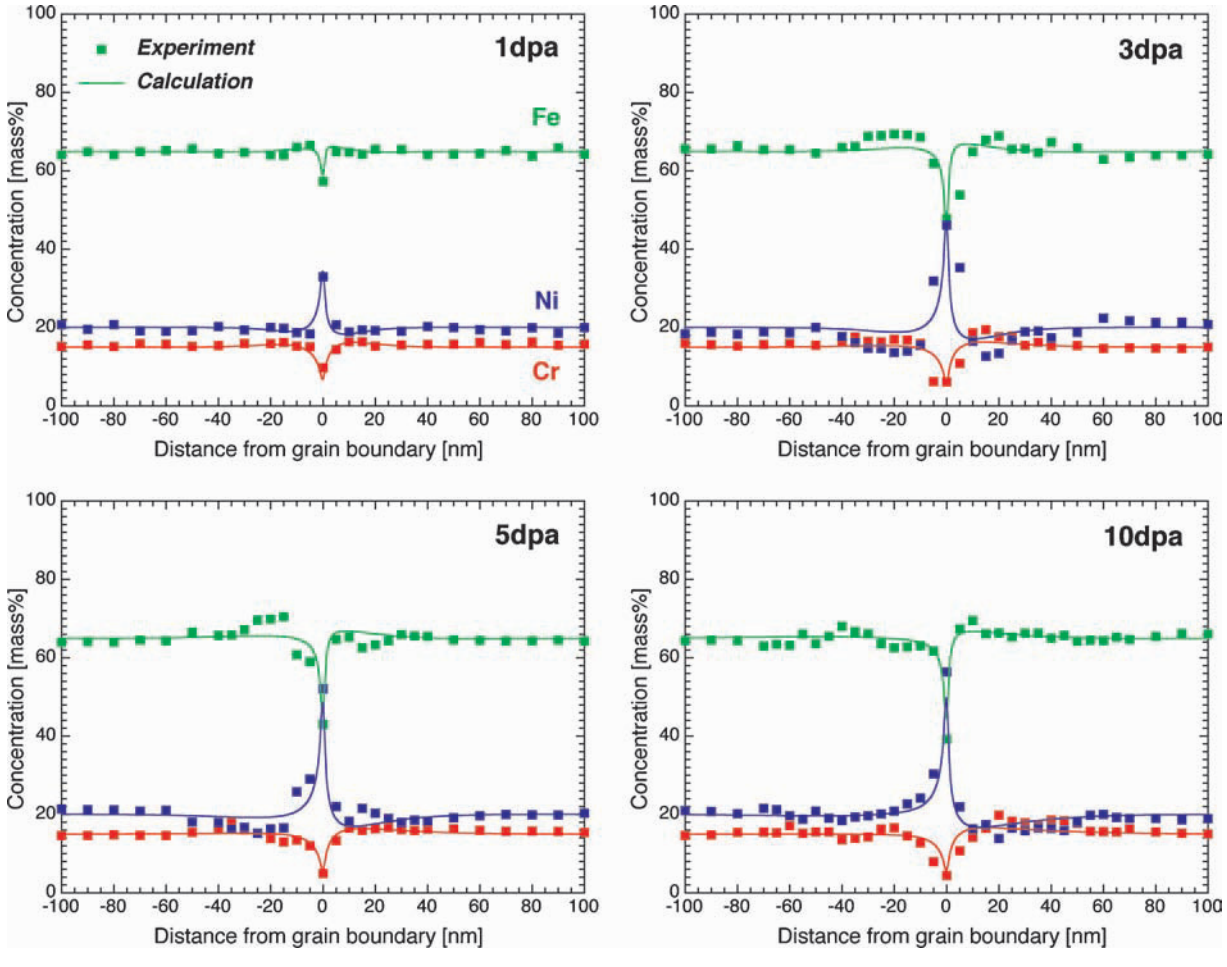

Figure 5 Concentration profile changes near an identical grain boundary after electron irradiation up to 10 dpa at 2×10^{-3} dpa/s and at 623 K. Solid lines are calculated results in the case of $\alpha_{v,i}. = 5 \times 10^{-8}$.

increasing of the migration distance. The good agreements were also obtained between the calculations and the experiments.

The rearrangement factor, $\alpha_{v,i}$, might be set less than 1×10^{-7} to reproduce the experimental RIS and RIGM data. This means that most of excess point defects annihilated to the grain boundaries do not contribute to the RIGM. In fact, grain boundary structural changes occur only at the micro steps on the boundary interfacial planes as shown in references 9 and 10. It is also important that the rearrangement factor would be a function of the grain boundary nature such as grain boundary types or misorientation angles. Further experimental knowledge should be needed to clarify the physical means of the rearrangement factor, $\alpha_{v,i}$.

4. Conclusions

In the present study, we performed the model calculation for the radiation-induced segregation (RIS) and the radiation-induced grain boundary migration (RIGM). In the present model, it was assumed that the RIS was induced by diffusional and annihilation processes of excess point defects at the grain boundary, and the RIGM occurred due to rearrangement process of atoms on one of the interfacial planes by annihilation of point defects. The calculated results indicated that the chromium depleted zone was expanded progressively by the RIGM and asymmetrical concentration profiles were observed around the grain boundary. The present model could explain the RIS behavior with or without grain boundary and good agreements with our previous experimental results were obtained.

Further experimental study on various aspects of the rearrangement factor $\alpha_{v,i}$, for example, the dependencies of irradiation temperature, kinds of irradiation particles, and the nature of grain boundaries, is needed. Some evidence of such dependencies on RIGM was recognized by the authors, but the details will be discussed elsewhere.

References

1. H. GROSS, H. P. FUCHS, H. J. LIPPERT and W. DAMBEITZ, *Nuclear Eng. and Design* **108** (1988) 433.
2. H. HANIEN and I. AHO-MANTILA, in "Proceedings of 3rd International Symposium on Environmental Degradation of Materials in Nuclear Power System-Water Reactors," edited by G. J. Thues and J. R. Weeks (The Metal Society of AIME, Warrendale, PA, 1988) p. 77.
3. J. F. BATES, R. W. POWELL and E. R. GILBERT, in "Effects of Radiation on Materials ASTM STP 725," edited by D. Kramer, H. R. Brager and J. S. Perrin (American Society for Testing and Materials, Philadelphia, PA, 1988) p. 713.
4. A. J. JACOBS, G. P. WOZADLO, K. NAKATA, T. OKADA and S. SUZUKI, *Corrosion* **50** (1994) 731.
5. S. M. BRUEMMER and E. P. SIMONEN, *ibid.* **50** (1994) 940.
6. H. TAKAHASHI, N. HASHIMOTO and S. WATANABE, *Ultramicroscopy* **56** (1994) 193.
7. S. WATANABE, N. SAKAGUCHI, N. HASHIMOTO and H. TAKAHASHI, *J. Nucl. Mater.* **224** (1995) 158.
8. S. WATANABE, N. SAKAGUCHI, N. HASHIMOTO, M. NAKAMURA, H. TAKAHASHI, C. NAMBA and N. Q. LAM, *J. Nucl. Mater.* **232** (1996) 133.
9. N. SAKAGUCHI, T. SHIBAYAMA, H. KINOSHITA and H. TAKAHASHI, *Philosophical Magazine Letters* **81** (2001) 691.
10. *Idem.*, *J. Nucl. Mater.* **307–311** (2002) 1003.
11. A. D. MARWICK, *ibid.* **135** (1985) 68.
12. N. SAKAGUCHI, S. WATANABE and H. TAKAHASHI, *ibid.* **239** (1996) 176.
13. *Idem.*, *Acta Mater.* **49** (2001) 1129.
14. S. WATANABE, Y. TAKAMATSU, N. SAKAGUCHI and H. TAKAHASHI, *J. Nucl. Mater.* **283–287** (2000) 152.
15. A. C. HINDMARCH, in "Scientific Computing," edited by R. S. Steplemann (North-Holland, Amsterdam, 1983) p. 55.